Equilibrium-Independent Stability Analysis for Distribution Systems With Lossy Transmission Lines

Wenqi Cui, *Graduate Student Member, IEEE*, and Baosen Zhang, *Member, IEEE*

***Abstract*—Power distribution systems are becoming much more active with increased penetration of distributed energy resources. Because of the intermittent nature of these resources, the stability of distribution systems under large disturbances and time-varying conditions is becoming a key issue in practical operations. Because the transmission lines in distribution systems are lossy, standard approaches in power system stability analysis do not readily apply. In this letter, the stability of lossy distribution systems is certified by breaking the network into subsystems. By looking at the equilibrium-independent passivity of each subsystem, the stability of the whole network is implied by the diagonal stability of the interconnection matrix. This analysis scales to large networked systems with time-varying equilibria. The proposed method gracefully extrapolates between lossless and lossy systems, and provides a simple yet effective approach to optimize control efforts with guaranteed stability regions. Case studies verify that the proposed method is much less conservative than existing approaches.**

***Index Terms*—Stability analysis, distribution systems, lossy transmission lines.**

I. Introduction

DISTRIBUTED energy resources (DERs) such as rooftop solar, electric vehicles and battery storage devices are increasingly entering the power distribution systems. These devices have intermittent outputs and often exhibit large and fast ramping variations, bringing larger disturbances to the system [1]. Therefore, stability of distribution systems under time-varying conditions and large disturbances is becoming a key question in their operations [2].

We are interested in the ability of a system to converge to an acceptable equilibrium following large disturbances [3], [4]. In power systems, this is often called transient stability analysis. Most of the time, transmission lines[1] are assumed to be lossless (i.e., the lines have no resistances). This significantly simplifies the mathematical analysis and allows for explicit constructions of energy functions for microgrids [5], [6], transmission systems [7], [8] and network-preserved differential-algebraic models [9], [10]. However, the transmission lines in distribution systems are lossy and have non-negligible resistances [11].

For lossy systems, transient stability becomes a much harder problem and remains open even for simplified models [2], [12]. A main difficulty is the lack of a good Lyapunov function (or energy function) [3], [4]. Existing explicit constructions require all the lines to have the same r/x ratios [6]. In more general cases, a classical approach is to use path-dependent integrals to construct Lyapunov functions, but these integrals are not always well-defined and rely on knowing the trajectories of the states [3]. Some works use linear matrix inequalities (LMIs) to find Lyapunov functions by relaxing sinusoidal AC power flow equations [2], [13]. These relaxations bound sinusoidal functions with linear or quadratic ones, but the bound can be loose and lead to conservative stability assessments. A candidate Lyapunov function can also be found via Sum Of Squares (SOS) programming techniques [14], but the computation complexity grows quickly with increased problem size. This makes the method difficult to scale to moderate or large systems. More recently, attempts have been made to learn a Lyapunov function parameterized by neural networks [12], [15]. However, it is challenging to verify that the learned neural networks satisfy Lyapunov conditions.

Apart from the challenges in scalability, existing approaches only apply a single equilibrium at a time [2], [12], [16]. Because of frequent changes to DERs' setpoints, equilibria are time-varying. Hence, it is essential to characterize stability for a set of possible equilibria. In addition, the power electronics on the DERs allow their damping coefficients to be adjusted [15], [17]. But optimizing these coefficients using existing approaches are nontrivial, since they involve solving complicated nonconvex problems or using trial and error.

This letter proposes a novel equilibrium-independent approach to transient stability analysis of lossy distribution systems, where we achieve scalability by breaking the network

Manuscript received 21 March 2022; revised 24 May 2022; accepted 6 June 2022. Date of publication 21 June 2022; date of current version 1 July 2022. This work was supported by the NSF under Grant ECCS-1930605 and Grant 2153937. Recommended by Senior Editor C. Prieur. *(Corresponding author: Wenqi Cui.)*

The authors are with the Department of Electrical and Computer Engineering, University of Washington Seattle, WA 98195 USA (e-mail: wenqicui@uw.edu; zhangbao@uw.edu).

Digital Object Identifier 10.1109/LCSYS.2022.3185027

[1]Power lines in the distribution system is also called transmission lines.

into subsystems. In particular, we consider the angle droop control for the power-electronic interfaces to drive voltage phase angles to their setpoints [2], [12]. Using the concept of equilibrium-independent passivity (EIP) [18], [19], we study the network stability with time-varying equilibrium points. Case studies verify that the proposed method is much less conservative and much more scalable to large systems compared with existing methods [2], [12]. The key contributions are as follows:

1) We propose a modular approach to study the angular stability of distribution network with time-varying equilibrium points and lossy transmission lines. Stability certification is reduced to checking the diagonal stability of the interconnection matrix over subsystems subject to EIP conditions. This provides a convex constraint on the damping coefficients and easily scales to large systems.
2) For lossy transmission lines, we design a tunable parameter that can serve to trade off between the control effort and the stability region. This method gracefully extrapolates between lossless and lossy systems, recovering the lossless results when the r/x ratio goes to 0.

II. Model and Problem Formulation

A. Power-Electronic Interfaced Distribution Systems

Consider a distribution system with n buses and m lines modelled as a connected graph $(\mathcal{N}, \mathcal{L})$, where each bus is equipped with a power-electronic interface [2], [12] Buses are indexed by $k \in \mathcal{N} := \{1, \ldots, n\}$. Lines are indexed by $l \in \mathcal{L} := \{n+1, \ldots, n+m\}$. Without loss of generality, we define the power flow from i to j to be the positive direction if $i < j$. We denote the interconnections between buses i, j and line l connecting them as $l \in \mathcal{B}_i^+$ and $l \in \mathcal{B}_j^-$, where $\mathcal{B}_i^+$ and $\mathcal{B}_j^-$ represents the line l leaving bus i and entering bus j, respectively.

We adopt the model proposed in [2] where angle and voltage droop control are utilized for real and reactive power sharing through power-electronic interfaces. Let δ_k and v_k be the voltage phase angle and voltage magnitude at bus $k \in \mathcal{N}$, and δ_k^*, v_k^* be their setpoint values set by distribution system operators (for more information on how the setpoints are chosen, see [2], [12]). Let p_k and q_k denote real and reactive power injections at bus k, and p_k^* and q_k^* be their setpoints. The dynamics of bus k are described by

$$\tau_{ak}\dot{\delta}_k = -d_{ak}(\delta_k - \delta_k^*) + \left(p_k^* - p_k\right) \tag{1a}$$

$$\tau_{vk}\dot{v}_k = -d_{vk}(v_k - v_k^*) + \left(q_k^* - q_k\right), \tag{1b}$$

where τ_{ak} and τ_{vk} are time constants for voltage phase angle and voltage magnitude at bus k, respectively. The parameters d_{ak} and d_{vk} are damping coefficients controlling power injected by inverters, and thus larger values correspond to larger control efforts. Importantly, the equilibria of the system come from the setpoints δ^* and v_k^*, which are time varying and not known ahead of time.

We follow the model in [2], [12] where $\tau_{vk} \gg \tau_{ak}$ by design. Then, the voltage v_k evolves much slower than the phase angle δ_k, hence the angle and voltage dynamics separates in timescale and v_k is typically assumed to be constant.

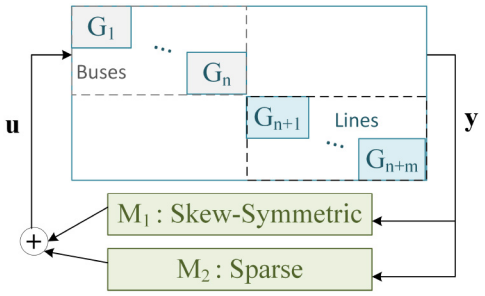

Fig. 1. Interconnection of buses (grey blocks) and transmission lines (blue blocks). The input and output of each subsystems are interconnected through the $\boldsymbol{y} = (\boldsymbol{M}_1 + \boldsymbol{M}_2)\boldsymbol{u}$, where $\boldsymbol{M}_1$ is skew-symmetric and $\boldsymbol{M}_2$ is sparse.

We therefore focus on the angle stability dynamics in (1a) and set $v_k = 1$ per unit in the rest of this letter.

Let g_l and b_l be the conductance and susceptance of the transmission line $l \in \mathcal{L}$, respectively. The active power flow in the line l from bus i to j is

$$p_l = g_l - g_l \cos(\delta_i - \delta_j) + b_l \sin(\delta_i - \delta_j), \tag{2}$$

which is the nonlinear AC power flow equation. We often use δ_{ij} as a shorthand for $\delta_i - \delta_j$. System operators calculate the setpoints such that p_k^* and δ_k^* satisfy the power flow equation for all $k \in \mathcal{N}$. A transmission line is called lossless if $g_l = 0$ and lossy otherwise. For distribution systems, g_l is typically not significantly smaller than b_l.

The buses are interconnected with transmission lines and the active power injected from bus k to the network is

$$p_k = \sum_{l \in \mathcal{B}_k^+} p_l - \sum_{l \in \mathcal{B}_k^-} p_l. \tag{3}$$

The dynamics of the system is described by (1a), (2) and (3). The transient stability of the system is defined as the ability to converge to the equilibrium points $\boldsymbol{\delta}^*$ from different initial conditions. Since equilibria are set by system operators, the system needs to be stable for multiple possible equilibria. In this letter, we adopt a modular approach to certify stability and design the damping coefficients d_{ak}'s, and show how it overcomes the challenges of existing approaches.

B. Stability Analysis Through a Modular Approach

The goal of this letter is to answer two key questions for the transient stability of distribution systems: *1) How large is the stability region?* and *2) What is the control effort needed to attain certain range of stability region?* To this end, we certify network-level stability by breaking the network into subsystems. Then by looking at the equilibrium-independent passivity (EIP) of each subsystems and their interconnections, the stability analysis scale to large networked systems with time-varying equilibrium points [19].

For each bus (1a) and each transmission line (2), we abstract them as a subsystem G_i with input $\boldsymbol{u}_i$ and output $\boldsymbol{y}_i$, which will be specified later in Section III. Fig. 1 shows the diagram for the connection of subsystems. The coupling of the input and output of each subsystems are described by $\boldsymbol{u} = \boldsymbol{M}\boldsymbol{y}$, where the matrix $\boldsymbol{M}$ is determined by interconnections of the system. We

show that $\boldsymbol{M}$ is the summation of a skew-symmetric matrix $\boldsymbol{M}_1$ and a sparse matrix $\boldsymbol{M}_2$. This enable us to obtain a compact and convex expression of stabilizing damping coefficients, which can easily be used for controller design.

If all the lines are lossless, the sparse component of $\boldsymbol{M}_2$ is zero and only the skew-symmetric part remains. Then standard results from EIP theory can be used to directly show the stability of the system, illustrating why lossless systems are simpler than lossy ones.

III. Modular Design of Subsystems

With the aim of network stability assessment through the passivity of subsystems, we study the abstraction of (1a)-(3) as subsystems of buses and lossy transmission lines and their input-output interconnections in this section.

A. Subsystems for Buses and Lossy Transmission Lines

The subsystem for the lossy transmission line $l \in \mathcal{L}$ leaving bus i and entering bus j is defined with the input $\boldsymbol{u}_l = \begin{bmatrix}\delta_i - \delta_j & \delta_j - \delta_i\end{bmatrix}^\top \in \mathbb{R}^2$ to be the angle differences from i to j and from j to i. The output $\boldsymbol{y}_l \in \mathbb{R}^2$ is defined to be the modified power flow from i to j and from j to i:

$$\begin{bmatrix} y_{l,1} \\ y_{l,2} \end{bmatrix} = \frac{1}{2}\begin{bmatrix} \big(g_l - g_l\cos(u_{l,1})\big)/\alpha_l + b_l \sin(u_{l,1}) \\ \big(g_l - g_l\cos(u_{l,2})\big)/\alpha_l + b_l \sin(u_{l,2}) \end{bmatrix} \tag{4a}$$

$$\begin{bmatrix} u_{l,1} \\ u_{l,2} \end{bmatrix} = \underbrace{\begin{bmatrix} 1 \\ -1 \end{bmatrix}}_{\Phi_{li}} \delta_i + \underbrace{\begin{bmatrix} -1 \\ 1 \end{bmatrix}}_{\Phi_{lj}} \delta_j \tag{4b}$$

where $\alpha_l > 0$ is a tunable scalar and we will study later in detail. At a high level, a larger α_l implies larger stability regions and larger stabilizing damping coefficients. The power flow (2) from bus i to j and that from bus j to i can be recovered by $p_{ij} = y_{l,1} - y_{l,2} + \alpha_l(y_{l,1} + y_{l,2})$ and $p_{ji} = -y_{l,1} + y_{l,2} + \alpha_l(y_{l,1} + y_{l,2})$, which will then serve as the input to the subsystem of buses. Stacking the inputs and outputs of lines gives $\boldsymbol{u}_\mathcal{L} = [\boldsymbol{u}_{n+1}^\top \cdots \boldsymbol{u}_{n+m}^\top] \in \mathbb{R}^{2m}$, and $\boldsymbol{y}_\mathcal{L} = [\boldsymbol{y}_{n+1}^\top \cdots \boldsymbol{y}_{n+m}^\top] \in \mathbb{R}^{2m}$. The matrix block $\Phi_{li} \coloneqq \begin{bmatrix} 1 & -1 \end{bmatrix}^\top$ and $\Phi_{lj} \coloneqq \begin{bmatrix} -1 & 1 \end{bmatrix}^\top$ are defined for the mapping from the output of the head i and the tail j to the input of line l, respectively.

The subsystem for bus k is defined with the input $u_k \in \mathbb{R}$ to be the power injection from connected transmission lines and the output $y_k \in \mathbb{R}$ to be the phase angle

$$\tau_k \dot{\delta}_k = -d_k(\delta_k - \delta_k^*) + \big(P_k^* + u_k\big) \tag{5a}$$

$$y_k = \delta_k \tag{5b}$$

$$u_k = \sum_{l \in \mathcal{B}_k^+} \underbrace{\begin{bmatrix} -1 & 1 \end{bmatrix}}_{\Phi_{kl}} y_l + \underbrace{\alpha_l \begin{bmatrix} -1 & -1 \end{bmatrix}}_{\Psi_{kl}} y_l + \sum_{l \in \mathcal{B}_k^-} \underbrace{\begin{bmatrix} 1 & -1 \end{bmatrix}}_{\Phi_{kl}} y_l + \underbrace{\alpha_l \begin{bmatrix} -1 & -1 \end{bmatrix}}_{\Psi_{kl}} y_l \tag{5c}$$

where the matrix block Φ_{kl} and Ψ_{kl} is defined for the mapping from the output of the subsystem for line $l \in \mathcal{L}$ to the input of the subsystem for bus $k \in \mathcal{N}$. The matrix block $\Phi_{kl} \coloneqq \begin{bmatrix} -1 & 1 \end{bmatrix}$ if $l \in \mathcal{B}_k^+$ and $\Phi_{kl} \coloneqq \begin{bmatrix} 1 & -1 \end{bmatrix}$ if $l \in \mathcal{B}_k^-$. The matrix block $\Phi_{kl} \coloneqq \begin{bmatrix} -\alpha_k & -\alpha_k \end{bmatrix}$ is defined uniformly for all line l that connects bus k. It will serve to constrain the minimum-effort damping coefficients that stabilize the system.

B. The Interconnection of Subsystems

To investigate the stability of the whole interconnected system, we stack the input/output vectors in sequence as $\boldsymbol{u} \coloneqq (\boldsymbol{u}_\mathcal{N}, \boldsymbol{u}_\mathcal{L}) \in \mathbb{R}^{n+2m}$ and $\boldsymbol{y} \coloneqq (\boldsymbol{y}_\mathcal{N}, \boldsymbol{y}_\mathcal{L}) \in \mathbb{R}^{n+2m}$. The mapping from the output of the bus $k \in \mathcal{N}$ to the input of the line $l \in \mathcal{L}$ is described by a matrix $\boldsymbol{\Phi}_{\mathcal{LN}} \in \mathbb{R}^{2m \times n}$, where the block in the $(2l-1)$-th, $2l$-th row and the k-th column is Φ_{lk} in (4). Similarly, the mapping from the output of the line $l \in \mathcal{L}$ to the input of the bus $k \in \mathcal{N}$ is described by the matrix $\boldsymbol{\Phi}_{\mathcal{NL}} \in \mathbb{R}^{n \times 2m}$, where the block in the k-th row and the $(2l-1)$ to $2l$-th column is Φ_{kl} in (5). The input-output dependent on α is represented in the matrix $\boldsymbol{\Psi} \in \mathbb{R}^{n \times 2m}$, where the block in the k-th row and the $(2l-1)$ to $2l$-th column is Ψ_{kl} in (5). Then, the interconnection of subsystems represented in (4) and (5) are compactly described by

$$\boldsymbol{u} = (\boldsymbol{M}_1 + \boldsymbol{M}_2)\boldsymbol{y} \tag{6}$$

where

$$\boldsymbol{M}_1 \coloneqq \begin{bmatrix} \boldsymbol{0}_{n\times n} & \boldsymbol{\Phi}_{\mathcal{NL}} \\ \boldsymbol{\Phi}_{\mathcal{LN}} & \boldsymbol{0}_{2m\times 2m} \end{bmatrix}, \boldsymbol{M}_2 \coloneqq \begin{bmatrix} \boldsymbol{0}_{n\times n} & \boldsymbol{\Psi} \\ \boldsymbol{0}_{2m\times n} & \boldsymbol{0}_{2m\times 2m} \end{bmatrix}.$$

Note that the matrix $\boldsymbol{\Phi}_{\mathcal{NL}}$ and $\boldsymbol{\Phi}_{\mathcal{LN}}$ is constituted by the blocks that satisfy $\Phi_{il} = -\Phi_{li}^\top$ for all $i \in \mathcal{N}$ and $l \in \mathcal{L}$, we have $\boldsymbol{\Phi}_{\mathcal{NL}} + \boldsymbol{\Phi}_{\mathcal{LN}}^\top = \boldsymbol{0}$ and thus $\boldsymbol{M}_1$ is skew-symmetric. The next section will show how the skew-symmetricity of $\boldsymbol{M}_1$ and the sparsity of $\boldsymbol{M}_2$ can be utilized for stability assessment of networked systems. We provide more detailed derivations and two examples in the longer online version of this letter [20].

IV. Compositional Stability Certification

A. Stability Region

The stability region is the set of initial states that converges to an equilibrium. Formally, it is defined as [9]:

Definition 1 (Stability Region): A dynamical system $\dot{\boldsymbol{\delta}} = \boldsymbol{f}_{\boldsymbol{u}}(\boldsymbol{\delta})$ is asymptotically stable around an equilibrium $\boldsymbol{\delta}^*$ if, $\forall \varphi > 0$, $\exists \theta > 0$ such that $\|\boldsymbol{\delta}(0) - \boldsymbol{\delta}^*\| < \theta$ implies $\|\boldsymbol{\delta}(t) - \boldsymbol{\delta}^*\| < \varphi$ and $\lim_{t\to\infty} \boldsymbol{\delta}(t) \longrightarrow \boldsymbol{\delta}^*$. The stability region of a stable equilibrium $\boldsymbol{\delta}^*$ is the set of all states $\boldsymbol{\delta}$ such that $\lim_{t\to\infty} \boldsymbol{\delta}(t) \longrightarrow \boldsymbol{\delta}^*$.

For nonlinear systems, it is very difficult to characterize the exact geometry of the whole stability region. This letter, and most others (see, e.g., [5], [6], [9]), attempt to find an inner approximation to the true stability region through Lyapunov's direct method. Correspondingly, the stability region is algebraically calculated by the states satisfying Lyapunov conditions $\mathcal{S}|_{V(\cdot)} = \{\boldsymbol{\delta} | V(\boldsymbol{\delta}) \geq 0, \dot{V}(\boldsymbol{\delta}) \leq 0\}$ with $V(\boldsymbol{\delta})$ be a Lyapunov function that equals zero at equilibrium. In the next subsections, we construct a Lyapunov function from equilibrium-independent passivity of subsystems, which will bring larger stability region than existing methods [2].

B. Equilibrium Independent Passivity

Equilibrium-independent passivity (EIP), characterized by a dissipation inequality referenced to an arbitrary equilibrium

input/output pair, allows one to ascertain passivity of the components without knowledge of the exact equilibrium [18]. The definition is given as follows [18], [19].

Definition 2 (Equilibrium-Independent Passivity): The system described by $\dot{\boldsymbol{\delta}} = f(\boldsymbol{\delta}, \boldsymbol{u}), \boldsymbol{y} = h(\boldsymbol{\delta}, \boldsymbol{u})$ is equilibrium-independent passive in a set $\boldsymbol{\delta} \in \mathcal{S}$ if, for every possible equilibrium $\boldsymbol{\delta}^* \in \mathcal{S}$, there exists a continuously-differentiable storage function $V_{\boldsymbol{\delta}^*} : \mathcal{S} \to \mathbb{R}_{\geq 0}$, such that $V_{\boldsymbol{\delta}^*}(\boldsymbol{\delta}^*) = 0$ and $\nabla_{\boldsymbol{\delta}} V_{\boldsymbol{\delta}^*}(\boldsymbol{\delta})^T f(\boldsymbol{\delta}, \boldsymbol{u}) \leq (\boldsymbol{u} - \boldsymbol{u}^*)^\top (\boldsymbol{y} - \boldsymbol{y}^*)$. If there further exists a positive scalar ϵ such that

$$\nabla_{\boldsymbol{\delta}} V_{\boldsymbol{\delta}^*}(\boldsymbol{\delta})^T f(\boldsymbol{\delta}, \boldsymbol{u}) \leq (\boldsymbol{u} - \boldsymbol{u}^*)^\top (\boldsymbol{y} - \boldsymbol{y}^*) - \epsilon (\boldsymbol{y} - \boldsymbol{y}^*)^\top (\boldsymbol{y} - \boldsymbol{y}^*), \quad (7)$$

then the system is strictly EIP.

In Section V, we will show that subsystems (5) corresponding to the bus $k \in \mathcal{N}$ is strictly EIP in the region $\mathcal{S}_k$ with $\epsilon_k = d_{ak}$ and the storage function $V_k(\boldsymbol{\delta}) = \frac{1}{2\tau_{ak}}(\delta_k - \delta_k^*)^2$. The subsystem (4) corresponding to the line $l \in \mathcal{L}$ is strictly EIP in the region $\mathcal{S}_l$ with $\epsilon_l = \frac{2\alpha_l}{\sqrt{g_l^2 + b_l^2 \alpha_l^2}}$ and the storage function $V_l(\boldsymbol{\delta}) = 0$. We denote $\boldsymbol{\epsilon}_{\mathcal{N}} := (\epsilon_1, \ldots, \epsilon_n)$, $\boldsymbol{\epsilon}_{\mathcal{L}} := (\epsilon_{n+1}\mathbf{1}_2, \ldots, \epsilon_{n+m}\mathbf{1}_2)$ for the EIP coefficients of buses and lines, and the diagonal matrices $\hat{\boldsymbol{\epsilon}}_{\mathcal{L}} := \operatorname{diag}(\boldsymbol{\epsilon}_{\mathcal{L}})$, $\hat{\boldsymbol{\epsilon}}_{\mathcal{N}} := \operatorname{diag}(\boldsymbol{\epsilon}_{\mathcal{N}})$ and $\hat{\boldsymbol{\epsilon}} := \operatorname{diag}(\boldsymbol{\epsilon}_{\mathcal{N}}, \boldsymbol{\epsilon}_{\mathcal{L}})$ that will be used in network stability certification. In particular, let $\boldsymbol{d}_{\mathcal{N}} := (d_{a1}, \ldots, d_{an})$, we have $\hat{\boldsymbol{\epsilon}}_{\mathcal{N}} = \operatorname{diag}(\boldsymbol{d}_{\mathcal{N}})$, which links stability certification with the control efforts.

C. Stability of Interconnected Systems

In this section we derive Lyapunov functions from the storage functions. We define the set $\mathcal{S} := \{\bigotimes_{i=1}^{n+m} \mathcal{S}_i\}$ to be the states that satisfy strictly EIP for each input-output pairs in all the subsystems. The next lemma allows us to construct Lyapunov functions for any equilibrium in $\mathcal{S}$. Consequently, $\mathcal{S}$ is an inner approximation of the stability region.

Lemma 1: Consider the networked system (4)-(6) with input $\boldsymbol{u}$ and output $\boldsymbol{y}$ that interconnected through $\boldsymbol{u} = \boldsymbol{M}\boldsymbol{y}$, where each input-output pair $\{u_i, y_i\}$ is locally strictly EIP with ϵ_i for $\boldsymbol{\delta} \in \mathcal{S}$. If there exists a diagonal matrix $\boldsymbol{C} \succ 0$ such that $\boldsymbol{C}(\boldsymbol{M} - \hat{\boldsymbol{\epsilon}}) + (\boldsymbol{M} - \hat{\boldsymbol{\epsilon}})^\top \boldsymbol{C} \prec 0$, then any equilibrium $\boldsymbol{\delta}^* \in \mathcal{S}$ is locally asymptotically stable.

Proof: The proof roughly follows [19]. For completeness, we provide the key steps. For the system (4)-(6), let the sum of the storage functions $V(\boldsymbol{\delta}) = \sum_{i=1}^{n+2m} c_i V_i(\boldsymbol{\delta})$ serve as a candidate Lyapunov function. Its time derivative is

$$\begin{aligned}
\dot{V}(\boldsymbol{\delta}) &= \sum_{i=1}^{n+2m} c_i \dot{V}_i(\boldsymbol{\delta}) \\
&\overset{①}{\leq} \sum_{i=1}^{n+2m} c_i \begin{bmatrix} u_i - u_i^* \\ y_i - y_i^* \end{bmatrix}^\top \begin{bmatrix} 0 & 1/2 \\ 1/2 & -\epsilon_i \end{bmatrix} \begin{bmatrix} u_i - u_i^* \\ y_i - y_i^* \end{bmatrix} \\
&= \frac{1}{2} \begin{bmatrix} \boldsymbol{u} - \boldsymbol{u}^* \\ \boldsymbol{y} - \boldsymbol{y}^* \end{bmatrix}^\top \begin{bmatrix} \mathbf{0} & \boldsymbol{C} \\ \boldsymbol{C} & -2\boldsymbol{C}\hat{\boldsymbol{\epsilon}} \end{bmatrix} \begin{bmatrix} \boldsymbol{u} - \boldsymbol{u}^* \\ \boldsymbol{y} - \boldsymbol{y}^* \end{bmatrix} \\
&= \frac{1}{2} [\boldsymbol{y} - \boldsymbol{y}^*]^\top \begin{bmatrix} \boldsymbol{M} \\ \boldsymbol{I} \end{bmatrix}^\top \begin{bmatrix} \mathbf{0} & \boldsymbol{C} \\ \boldsymbol{C} & -2\boldsymbol{C}\hat{\boldsymbol{\epsilon}} \end{bmatrix} \begin{bmatrix} \boldsymbol{M} \\ \boldsymbol{I} \end{bmatrix} [\boldsymbol{y} - \boldsymbol{y}^*] \\
&= \frac{1}{2} (\boldsymbol{y} - \boldsymbol{y}^*)^\top \Big(\boldsymbol{C}(\boldsymbol{M} - \hat{\boldsymbol{\epsilon}}) + (\boldsymbol{M} - \hat{\boldsymbol{\epsilon}})^\top \boldsymbol{C} \Big) (\boldsymbol{y} - \boldsymbol{y}^*), \quad (8)
\end{aligned}$$

where ① follows from the conditions on EIP in (7). Because $\boldsymbol{y} = \boldsymbol{y}^*$ if and only if $\boldsymbol{\delta} = \boldsymbol{\delta}^*$, $\boldsymbol{C}(\boldsymbol{M} - \hat{\boldsymbol{\epsilon}}) + (\boldsymbol{M} - \hat{\boldsymbol{\epsilon}})^\top \boldsymbol{C} \prec 0$ implies $\dot{V}(\boldsymbol{\delta}) < 0$ for $\boldsymbol{y} \neq \boldsymbol{y}^*$. Hence $V(\boldsymbol{\delta})$ is a valid Lyapunov function for $\boldsymbol{\delta} \in \mathcal{S}$, and an equilibrium $\boldsymbol{\delta}^* \in \mathcal{S}$ is locally asymptotically stable. ■

The LMI in Lemma 1 is not jointly convex in $\boldsymbol{d}_{\mathcal{N}}$ and $\boldsymbol{C}$. Setting $\boldsymbol{C} = \boldsymbol{I}$ gives a simple convex condition on $\boldsymbol{d}_{\mathcal{N}}$.

Theorem 1 (Local Exponential Stability): If the damping coefficients satisfy $\operatorname{diag}(\boldsymbol{d}_{\mathcal{N}}) \succ \frac{1}{4}\boldsymbol{\Psi}\hat{\boldsymbol{\epsilon}}_{\mathcal{L}}^{-1}\boldsymbol{\Psi}^\top$, an equilibrium $\boldsymbol{\delta}^* \in \mathcal{S}$ of the system (1)-(3) is locally exponentially stable.

Proof: This theorem follows from picking $\boldsymbol{C}$ to be the identity matrix. In this case, the condition in Lemma 1 becomes $(\boldsymbol{M}^\top + \boldsymbol{M} - 2\hat{\boldsymbol{\epsilon}}) \prec 0$. From (6), $\boldsymbol{M} = \boldsymbol{M_1} + \boldsymbol{M_2}$, and using the fact that $\boldsymbol{M_1}$ is skew symmetric, and expanding $\hat{\boldsymbol{\epsilon}} := \operatorname{diag}(\boldsymbol{d}_{\mathcal{N}}, \boldsymbol{\epsilon}_{\mathcal{L}})$, we have

$$\dot{V}(\boldsymbol{\delta}) = \big(\boldsymbol{y} - \boldsymbol{y}^*\big)^\top \begin{bmatrix} -\operatorname{diag}(\boldsymbol{d}_{\mathcal{N}}) & \frac{1}{2}\boldsymbol{\Psi} \\ \frac{1}{2}\boldsymbol{\Psi} & -\hat{\boldsymbol{\epsilon}_{\mathcal{L}}} \end{bmatrix} \big(\boldsymbol{y} - \boldsymbol{y}^*\big). \quad (9)$$

To certify exponential stability, we need to find a scalar $\sigma > 0$, such that $\dot{V}(\boldsymbol{\delta}) < -\sigma V(\boldsymbol{\delta})$. Since the Lyapunov function $V(\boldsymbol{\delta}) = \sum_{i=1}^{n+2m} c_i V_i(\boldsymbol{\delta})$ is

$$\begin{aligned}
V(\boldsymbol{\delta}) &= \sum_{i=1}^{n} \frac{1}{2\tau_{ai}} \big(\delta_i - \delta_i^*\big)^2 \\
&= \big(\boldsymbol{y} - \boldsymbol{y}^*\big)^\top \begin{bmatrix} \frac{1}{2}\operatorname{diag}(\boldsymbol{\tau})^{-1} & \mathbf{0}_{n\times 2m} \\ \mathbf{0}_{2m\times n} & \mathbf{0}_{2m\times 2m} \end{bmatrix} \big(\boldsymbol{y} - \boldsymbol{y}^*\big),
\end{aligned}$$

then $\dot{V}(\boldsymbol{\delta}) < -\sigma V(\boldsymbol{\delta})$ is equivalent to

$$\begin{bmatrix} 2\operatorname{diag}(\boldsymbol{d}_{\mathcal{N}}) - \sigma \operatorname{diag}(\boldsymbol{\tau})^{-1} & -\boldsymbol{\Psi} \\ -\boldsymbol{\Psi} & 2\hat{\boldsymbol{\epsilon}_{\mathcal{L}}} \end{bmatrix} \succ 0. \quad (10)$$

By definition, $\hat{\boldsymbol{\epsilon}_{\mathcal{L}}} \succ 0$ and Schur complement gives

$$\Big(2\operatorname{diag}(\boldsymbol{d}_{\mathcal{N}}) - \sigma \operatorname{diag}(\boldsymbol{\tau})^{-1}\Big) - \frac{1}{2}\boldsymbol{\Psi}\hat{\boldsymbol{\epsilon}_{\mathcal{L}}}^{-1}\boldsymbol{\Psi}^\top \succ 0.$$

If $\operatorname{diag}(\boldsymbol{d}_{\mathcal{N}}) \succ \frac{1}{4}\boldsymbol{\Psi}\hat{\boldsymbol{\epsilon}}_{\mathcal{L}}^{-1}\boldsymbol{\Psi}^\top$, then any σ satisfying $0 < \sigma < \lambda_{\min}(2\operatorname{diag}(\boldsymbol{d}_{\mathcal{N}}) - \frac{1}{2}\boldsymbol{\Psi}\hat{\boldsymbol{\epsilon}}_{\mathcal{L}}^{-1}\boldsymbol{\Psi}^\top) \min_{i=1}^{n} \tau_{ai}$ guarantees (10) and $\boldsymbol{\delta}^*$ is locally exponentially stable. ■

Note that the damping coefficients obtained in Theorem 1 is derived by setting $\boldsymbol{C} = \boldsymbol{I}$, thus the region of stabilizing damping coefficients $\operatorname{diag}(\boldsymbol{d}_{\mathcal{N}}) \succeq \frac{1}{4}\boldsymbol{\Psi}\hat{\boldsymbol{\epsilon}}_{\mathcal{L}}^{-1}\boldsymbol{\Psi}^\top$ is a subset of that verified through $\boldsymbol{C}(\boldsymbol{M} - \hat{\boldsymbol{\epsilon}}) + (\boldsymbol{M} - \hat{\boldsymbol{\epsilon}})^\top \boldsymbol{C} \prec 0$. We will show in the case study that the damping coefficients obtained by $\operatorname{diag}(\boldsymbol{d}_{\mathcal{N}}) \succeq \frac{1}{4}\boldsymbol{\Psi}\hat{\boldsymbol{\epsilon}}_{\mathcal{L}}^{-1}\boldsymbol{\Psi}^\top$ is already much less conservative compared with existing LMIs-based methods [2].

V. Controller Design From EIP of Subsystems

In this section, we prove the strictly EIP of the subsystems in (4) and (5). The system stability region is built from the angles that stabilize each of the subsystems. We also show how each stability region can be tuned to tradeoff with the size of the stabilizing damping coefficients.

A. Strictly EIP of Lossy Transmission Lines and Buses

The next Lemma shows that the subsystem (4) of each lossy transmission line $l \in \mathcal{L}$ is strictly EIP for a region $\mathcal{S}_l$.

Lemma 2 (EIP of Lossy Lines): The lossy transmission line l from bus i to j represented by (4) is strictly EIP with $\epsilon_l = \frac{2\alpha_l}{\sqrt{g_l^2 + b_l^2 \alpha_l^2}}$ for all the possible equilibriums δ_{ij}^* in the set $\mathcal{S}_l = \{\delta_{ij}^* | -\arctan(b_l\alpha_l/g_l) \leq \delta_{ij}^* \leq \arctan(b_l\alpha_l/g_l)\}$.

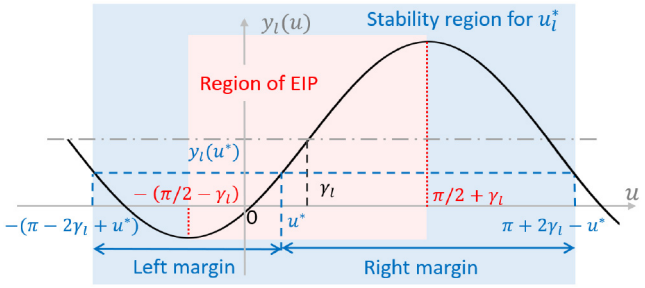

Fig. 2. The region of EIP $\boldsymbol{\mathcal{S}}_l$ is computed by $y_l'(u) \geq 0$ and is labeled in red. The stability region for an equilibrium u^* is the areas that $y_l(u) - y_l(u^*)$ and $u - u^*$ has the same sign. The stability region is in blue and its intersection for all equilibrium $u^* \in \boldsymbol{\mathcal{S}}_l$ is the region of EIP in red.

First we note that if $g_l = 0$, then the subsystem (4) is strictly EIP in $\delta_{ij}^* \in (-\frac{\pi}{2}, \frac{\pi}{2})$ for any $\alpha_l > 0$. In particular, $\boldsymbol{\Psi}$ can be made arbitrarily close to $\mathbf{0}$ and $\mathrm{diag}(\boldsymbol{d}_{\mathcal{N}}) \succ \frac{1}{4}\boldsymbol{\Psi}\hat{\boldsymbol{\epsilon}}_{\mathcal{L}}^{-1}\boldsymbol{\Psi}^\top$ for any $\boldsymbol{d}_{\mathcal{N}} > 0$. Namely, $\delta_{ij}^* \in (-\frac{\pi}{2}, \frac{\pi}{2})$ is stable for any positive damping coefficients. This recovers the observations for lossless transmission lines [7].

For lossy transmission line with $g_l > 0$, Lemma 2 shows that α_l trades off between the size of $\mathcal{S}_l$ and passivity: a larger α_l enlarges $\mathcal{S}_l$ but also increases the bound $\frac{1}{4}\boldsymbol{\Psi}\hat{\boldsymbol{\epsilon}}_{\mathcal{L}}^{-1}\boldsymbol{\Psi}^\top$ that requires larger damping. The proof is given below.

Proof: The subsystem (4) is a memoryless system, where $y_{l,1}$ and $y_{l,2}$ is a function of the input $u_{l,1} = \delta_{ij}$ and $u_{l,2} = -\delta_{ij}$, respectively. Hence, it suffices to consider the function

$$\begin{aligned} y_l(u) &= \frac{g_l - g_l\cos(u)}{2\alpha_l} + \frac{b_l}{2}\sin(u) \\ &= \frac{g_l}{2\alpha_l} + \frac{\sqrt{g_l^2 + b_l^2\alpha_l^2}}{2\alpha_l}\sin(u - \gamma_l), \end{aligned} \tag{11}$$

when $u = \delta_{ij}$ and $u = -\delta_{ij}$, respectively. The constant $\gamma_l = \arctan(\frac{g_l}{b_l\alpha_l}) \in (0, \pi/2)$ horizontally shift the function $y_l(u)$ as shown in Fig. 2 and thus affect the range of δ_{ij} satisfying strictly EIP. For the memoryless system (11), we take the storage function to be zero and then the condition for strict passivity is [19]

$$\big(u - u^*\big)\big(y_l(u) - y_l(u^*)\big) - \epsilon_l\big(y_l(u) - y_l(u^*)\big)^2 \geq 0, \tag{12}$$

which holds for any equilibrium if and only if $y_l'(u) \in [0, \frac{1}{\epsilon_l}]$. To this end, setting $\epsilon_l = \frac{2\alpha}{\sqrt{g^2+b^2\alpha^2}}$ guarantees that $y_l'(u) \leq \frac{1}{\epsilon_l}$. Then $y_l'(u) \geq 0$ is guaranteed for the region $u \in [-\frac{\pi}{2} + \gamma_l, \frac{\pi}{2} + \gamma_l]$, which is labeled in red in Fig. 2.

Substituting $u = \delta_{ij}$ and $u = -\delta_{ij}$ gives $-\frac{\pi}{2} \leq \delta_{ij} - \gamma_l \leq \frac{\pi}{2}$ and $-\frac{\pi}{2} \leq -\delta_{ij} - \gamma_l \leq \frac{\pi}{2}$, respectively. Taking the intersection, the angle difference satisfying strictly EIP is $\delta_{ij} \in [-\frac{\pi}{2} + \gamma_l, \frac{\pi}{2} - \gamma_l]$, which is equivalent to $\delta_{ij} \in [-\arctan(b_l\alpha_l/g_l), \arctan(b_l\alpha_l/g_l)]$. ∎

Lemma 3 (EIP of buses): Bus k represented by (5) is strictly EIP with $\epsilon_k = d_{ak}$ for all equilibria $\delta_k^* \in \mathbb{R}$.

This Lemma shows that the subsystem of buses is strictly EIP for all the possible equilibrium of angles. It follows directly from the definitions and the proof is given in the longer online version of this letter [20].

B. Sizing Stability Regions

The equilibrium-independent stability guarantees that any equilibrium in the set $\mathcal{S}$ is exponentially stable. Naturally, it is of interest to control the size of the stability region $\mathcal{S}$. The next theorem shows how the parameter α should be chosen if the stability region need to meet a prescribed size.

Theorem 2 (Tuning α for Stability Region): For the line l from bus i to j with an equilibrium $\delta_{ij}^* \in \mathcal{S}_l$, the stability region is $\mathcal{S}_l|_{\boldsymbol{\delta}^*} = \{\delta_{ij} | -2\arctan(b_l\alpha_l/g_l) - \delta_{ij}^* \leq \delta_{ij} \leq 2\arctan(b_l\alpha_l/g_l) - \delta_{ij}^*\}$. If $\alpha_l \geq \frac{g_l\tan(|\delta_{ij}^*| + \beta_l/2)}{b_l}$ for a constant $0 < \beta_l < \pi - 2|\delta_{ij}^*|$, then the system is guaranteed to be stable around the equilibrium δ_{ij}^* with at least the margin of β_l, i.e., $[\delta_{ij}^* - \beta_l, \delta_{ij}^* + \beta_l] \subset \mathcal{S}_l|_{\boldsymbol{\delta}^*}$.

Note that if varying δ_{ij}^* in the set $\mathcal{S}_l = \{\delta_{ij}^* | -\arctan(b_l\alpha_l/g_l) \leq \delta_{ij}^* \leq \arctan(b_l\alpha_l/g_l)\}$, the intersection of $\mathcal{S}_l|_{\boldsymbol{\delta}^*}$ is exactly $\mathcal{S}_l$. Hence, the region of equilibrium-independent stability can also be understood as the intersection of the stability region for all the possible equilibrium.

Proof: The stability certification (8)-(10) holds as long as the inequality (7) holds. For a certain equilibrium $\boldsymbol{\delta}^*$, we define the stability region $\mathcal{S}_l|_{\boldsymbol{\delta}^*}$ to be the angles satisfying the inequality (7). This condition is equivalent to certifying (12) for $u = \delta_{ij}$ and $u = -\delta_{ij}$ when fixing $u^* = \delta_{ij}^*$. Note that $\epsilon_l = \frac{2\alpha}{\sqrt{g^2+b^2\alpha^2}}$ gives $y_l'(u) \leq \frac{1}{\epsilon_l}$, then condition (12) is satisfied as long as $y_l(u) - y_l(u^*)$ is the same sign as $u - u^*$ for both $u = \delta_{ij}$ and $u = -\delta_{ij}$.

The signs of $y_l(u) - y_l(u^*)$ and $u - u^*$ are the same when $u \in [-\pi + 2\gamma_l - u^*, \pi + 2\gamma_l - u^*]$. This region is labeled in blue in Fig. 2, which is larger than the region of EIP shown in red. For $u = \delta_{ij}$ and $u = -\delta_{ij}$, we have $\delta_{ij} \in [-\pi + 2\gamma_l - \delta_{ij}^*, \pi + 2\gamma_l - \delta_{ij}^*]$, and $-\delta_{ij} \in [-\pi + 2\gamma_l + \delta_{ij}^*, \pi + 2\gamma_l + \delta_{ij}^*]$, respectively. The intersection gives the region

$$\mathcal{S}_l|_{\boldsymbol{\delta}^*} = \{\delta_{ij} | -\pi + 2\gamma_l - \delta_{ij}^* \leq \delta_{ij} \leq \pi - 2\gamma_l - \delta_{ij}^*\}. \tag{13}$$

and thus $[\delta_{ij}^* - \beta_l, \delta_{ij}^* + \beta_l] \subset \mathcal{S}_l|_{\boldsymbol{\delta}^*}$ yields

$$-\pi + 2\gamma_l - \delta_{ij}^* \leq \delta_{ij}^* - \beta_l \leq \delta_{ij}^* + \beta_l \leq \pi - 2\gamma_l - \delta_{ij}^*,$$

which gives $\frac{\pi}{2} - \gamma_l \geq |\delta_{ij}^*| + \frac{\beta_l}{2}$. Equivalently, $\arctan(\frac{b_l\alpha}{g_l}) \geq |\delta_{ij}^*| + \frac{\beta_l}{2}$ and thus we require $\alpha_l \geq \frac{g_l\tan(|\delta_{ij}^*| + \beta_l/2)}{b_l}$. ∎

Theorems 1 and 2 provide a way of optimizing over the damping coefficients while guaranteeing the size of the stability region. Suppose the margin of stable angle difference is $\beta_l \in [0, \pi - 2|\delta_{ij}^*|]$ for $l \in \mathcal{L}$, we define $\alpha_l = \frac{g_l\tan(|\delta_{ij}^*| + \beta_l/2)}{b_l}$. Thus, $\epsilon_l = \frac{2\alpha_l}{\sqrt{g_l^2+b_l^2\alpha_l^2}}$ and $\boldsymbol{\Psi}$ is determined by α_l's through (5b). To minimize the damping coefficients (related to hardware costs [17]), we can solve

$$\min_{\boldsymbol{d}_{\mathcal{N}}} \ \|\boldsymbol{d}_{\mathcal{N}}\|_2 \tag{14a}$$

$$\text{s.t.} \ \ \mathrm{diag}(\boldsymbol{d}_{\mathcal{N}}) \succ \frac{1}{4}\boldsymbol{\Psi}\hat{\boldsymbol{\epsilon}}_{\mathcal{L}}^{-1}\boldsymbol{\Psi}^\top, \tag{14b}$$

which is a convex problem. The Pareto-front of the least-cost damping coefficients and the size of stability region can be computed by varying α, quantifying the trade-off between control efforts and stability regions.

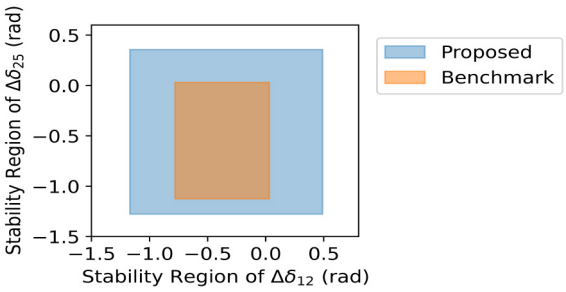

Fig. 3. Stability regions of $\Delta\delta_{12}$ and $\Delta\delta_{25}$ under the same damping coefficients. The proposed approach finds a larger stability region.

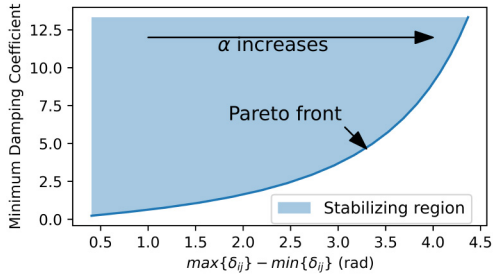

Fig. 4. Pareto-front of the width of the stability region and the minimum stabilizing damping coefficients by varying α from 0.1 to 2 in line 1.

VI. Case Study

Case studies are conducted on the IEEE 123-node test feeder [11]. Since existing LMIs-based and neural network-based methods all partition the network into a 5-bus system to alleviate computational issues [2], [12], we first work with this 5-bus system to compared against these baselines. Then, we directly work with the original 123-node feeder to show that the proposed approach can scale to large systems.

A. Comparison With LMIs-Based Stability Assessment

We first compare with existing LMI-based transient stability assessment found in [2]. Under the same damping coefficients, Fig. 3 compares the stability regions of two lines calculated by our proposed method and the benchmark in [2]. The angle difference δ_{ij} relative to an equilibrium for the line connecting bus i and j is labeled as $\Delta\delta_{ij} \coloneqq \delta_{ij} - \delta_{ij}^*$. Our proposed approach attains much larger stability region.

From the other direction, if we fix the size of the stability regions, (14) can be solved to find the stabilizing damping coefficients. This is in contrast to existing methods, where damping coefficients are found through exhaustive searches.

B. Performance on Large Systems

To verify the performance of the proposed method on larger systems, we further simulate on the original 123-node test feeder. Fig. 4 shows the Pareto-front of the width of the stability region and the least-norm stabilizing damping coefficient by varying α from 0.1 to 2 in the line 1. This quantifies the trade-off between enlarging the stability region and minimizing control efforts. More simulation results can be found in the longer online version of this letter [20].

VII. Conclusion

This letter proposes a modular approach for transient stability analysis of distribution systems with lossy transmission lines and time-varying equilibria. Network stability is decomposed into the strictly EIP of subsystems and the diagonal stability of the interconnection matrix. This in turn provides a simple yet effective approach to optimize damping coefficients with guaranteed stability regions. Case studies show that the proposed method is less conservative compared with existing approaches and can scale to large systems. Incorporating the voltage and the frequency response with conventional machines are important future directions for us.

References

[1] S. C. Ross and J. L. Mathieu, "A method for ensuring a load aggregator's power deviations are safe for distribution networks," *Electr. Power Syst. Res.*, vol. 189, Dec. 2020, Art. no. 106781.
[2] Y. Zhang and L. Xie, "A transient stability assessment framework in power electronic-interfaced distribution systems," *IEEE Trans. Power Syst.*, vol. 31, no. 6, pp. 5106–5114, Nov. 2016.
[3] H.-D. Chiang, "Study of the existence of energy functions for power systems with losses," *IEEE Trans. Circuits Syst.*, vol. 36, no. 11, pp. 1423–1429, Nov. 1989.
[4] S. Sastry, *Nonlinear Systems: Analysis, Stability, and Control*, vol. 10. New York, NY, USA: Springer, 2013.
[5] J. Schiffer, R. Ortega, A. Astolfi, J. Raisch, and T. Sezi, "Conditions for stability of droop-controlled inverter-based microgrids," *Automatica*, vol. 50, no. 10, pp. 2457–2469, 2014.
[6] C. De Persis and N. Monshizadeh, "Bregman storage functions for microgrid control," *IEEE Trans. Autom. Control*, vol. 63, no. 1, pp. 53–68, Jan. 2018.
[7] W. Cui, Y. Jiang, and B. Zhang, "Reinforcement learning for optimal primary frequency control: A Lyapunov approach," 2021, *arXiv:2009.05654*.
[8] P. W. Sauer, M. A. Pai, and J. H. Chow, *Power System Dynamics and Stability: With Synchrophasor Measurement and Power System Toolbox*. Hoboken, NJ, USA: Wiley, 2017.
[9] H.-D. Chiang, *Direct Methods for Stability Analysis of Electric Power Systems: Theoretical Foundation, BCU Methodologies, and Applications*. Hoboken, NJ, USA: Wiley, 2011.
[10] C. De Persis, N. Monshizadeh, J. Schiffer, and F. Dörfler, "A Lyapunov approach to control of microgrids with a network-preserved differential-algebraic model," in *Proc. IEEE 55th Conf. Decis. Control (CDC)*, 2016, pp. 2595–2600.
[11] W. H. Kersting, "Radial distribution test feeders," *IEEE Trans. Power Syst.*, vol. 6, no. 3, pp. 975–985, Aug. 1991.
[12] T. Huang, S. Gao, and L. Xie, "A neural Lyapunov approach to transient stability assessment of power electronics-interfaced networked microgrids," *IEEE Trans. Smart Grid*, vol. 13, no. 1, pp. 106–118, Jan. 2022.
[13] T. L. Vu and K. Turitsyn, "Lyapunov functions family approach to transient stability assessment," *IEEE Trans. Power Syst.*, vol. 31, no. 2, pp. 1269–1277, Mar. 2016.
[14] M. Anghel, F. Milano, and A. Papachristodoulou, "Algorithmic construction of Lyapunov functions for power system stability analysis," *IEEE Trans. Circuits Syst. I, Reg. Papers*, vol. 60, no. 9, pp. 2533–2546, Sep. 2013.
[15] W. Cui and B. Zhang, "Lyapunov-regularized reinforcement learning for power system transient stability," *IEEE Control Syst. Lett.*, vol. 6, pp. 974–979, 2021.
[16] X. Miao and M. D. Ilić, "Modeling and distributed control of microgrids: A negative feedback approach," in *Proc. IEEE 58h Conf. Decis. Control (CDC)*, 2019, pp. 1937–1944.
[17] B. B. Johnson, S. V. Dhople, A. O. Hamadeh, and P. T. Krein, "Synchronization of parallel single-phase inverters with virtual oscillator control," *IEEE Trans. Power Electron.*, vol. 29, no. 11, pp. 6124–6138, Nov. 2014.
[18] G. H. Hines, M. Arcak, and A. K. Packard, "Equilibrium-independent passivity: A new definition and numerical certification," *Automatica*, vol. 47, no. 9, pp. 1949–1956, 2011.
[19] M. Arcak, C. Meissen, and A. Packard, *Networks of Dissipative Systems: Compositional Certification of Stability, Performance, and Safety*. Cham, Switzerland: Springer, 2016.
[20] W. Cui and B. Zhang, "Equilibrium-independent stability analysis for distribution systems with lossy transmission lines," 2022, *arXiv:2203.04580*.